Supplemental data

Chemistry

All reagents were used directly as obtained commercially from Sigma-Aldrich (St. Louis, MO). Nor-fluoro-FNDP was prepared as described previously (*1*). Column flash chromatography was carried out using E. Merck silica gel 60F (230–400 mesh) (Sigma-Aldrich). ^{1}H NMR spectra were recorded on a Bruker-500 MHz NMR spectrometer (Billerica, Massachusetts), in $CDCl_3$ (referenced to internal Me_4Si at δ_H 0 ppm). The high performance liquid chromatography (HPLC) system consisted of two Varian ProStar pumps (Palo Alto, California), a single Rheodyne Model 7725i manual injector, a ProStar 325 UV-Vis variable wavelength detector, and a BioScan Flow-Count radioactivity detector (Poway, California). Analytical and semi-preparative chromatography was performed using Phenomenex Luna C-18 10 µm columns (4.6 x 250 mm and 10 x 250 mm, respectively) (Torrance, California).

N-(3,3-diphenylpropyl)-6-fluoronicotinamide (FNDP)

3,3-Diphenylpropan-1-amine (105.5 mg, 0.5 mmol) was added to a solution of 6-fluoronicotinic acid (70.5 mg, 0.5 mmol) in 3 mL *N*,*N*-dimethylformamide and followed by the addition of 1-hydroxybenzotriazole (135 mg, 1 mmol), 1-[3-(dimethylamino)propyl]-3-ethylcarbodiimde hydrochloride (191 mg, 1 mmol), and diisopropylethylamine (195.5 mg, 1.5 mmol). The reaction was stirred at room temperature for 48 h, the solvent was evaporated under vacuum and the residue was separated by flash LC (silica gel, hexane-ethylacetate 5:1 → 2:1) to give the desired product, FNDP (121 mg, 72%).

^{1}H NMR ($CHCl_3$-d_3, 500 MHz) δ 8.32 (d, *J*=2.5 Hz, 1H), 8.10-8.06 (m, 1H), 7.27-7.24 (m, 8H), 7.25 (m, 2H), 7.01-6.98(m, 1H), 5.92 (broad s, 1H), 4.07 (t, *J*=8Hz, 1H), 3.57 (m, 2H), 2.48 (m, 2H).

6-Bromo-*N*-(3,3-diphenylpropyl)nicotinamide (precursor-FNDP)

Precursor-FNDP was prepared similarly to FNDP using 6-bromonicotinic acid as the starting material. Yield: 59%. ^{1}H NMR ($CHCl_3$-d_3, 500 MHz) δ 8.45 (d, *J*=2.5 Hz, 1H), 7.79 (m, 1H), 7.56 (d, *J*=8Hz, 1H), 7.37-7.32 (m, 8H), 7.27-7.24 (m, 2H), 5.92 (broad s, 1H), 4.07 (t, *J*=9Hz, 1H), 3.56 (m, 2H), 2.49 (m, 2H).

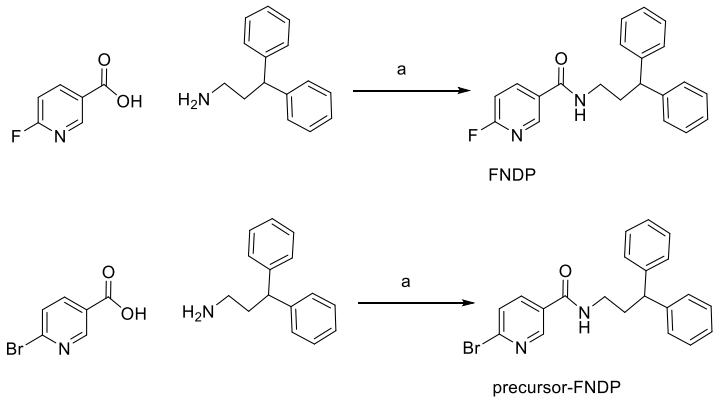

Supplemental Figure 1. Synthesis of FNDP and precursor-FNDP for radiolabeling of ^{18}F-FNDP. Reagents and conditions: (a) 1-[3-(dimethylamino)propyl]-3-ethylcarbodiimde, HOBt, DIPEA, DMF, room temperature.

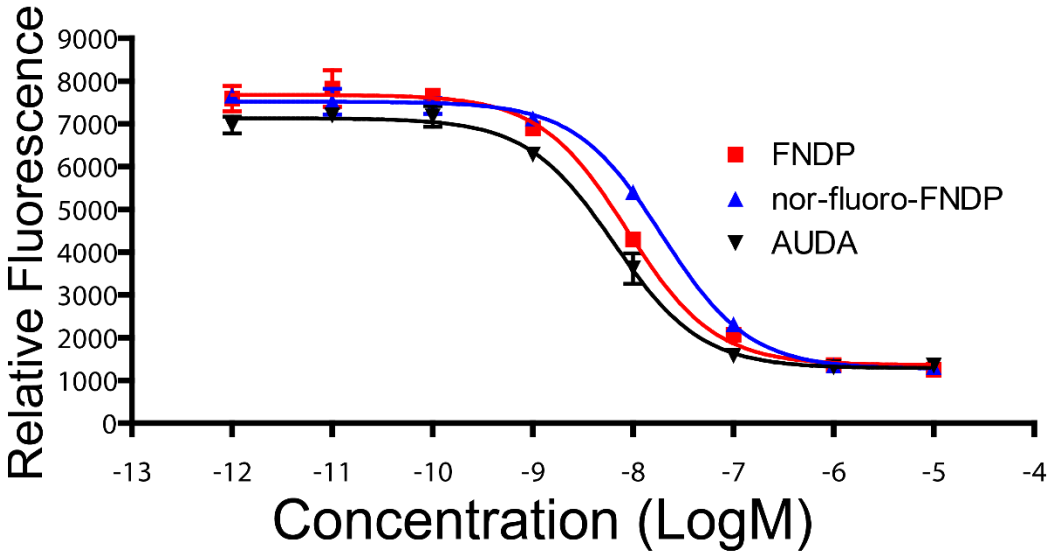

Supplemental Figure 2. FNDP demonstrated low nanomolar inhibitory activity against sEH, comparable to that of AUDA and nor-fluoro-FNDP.

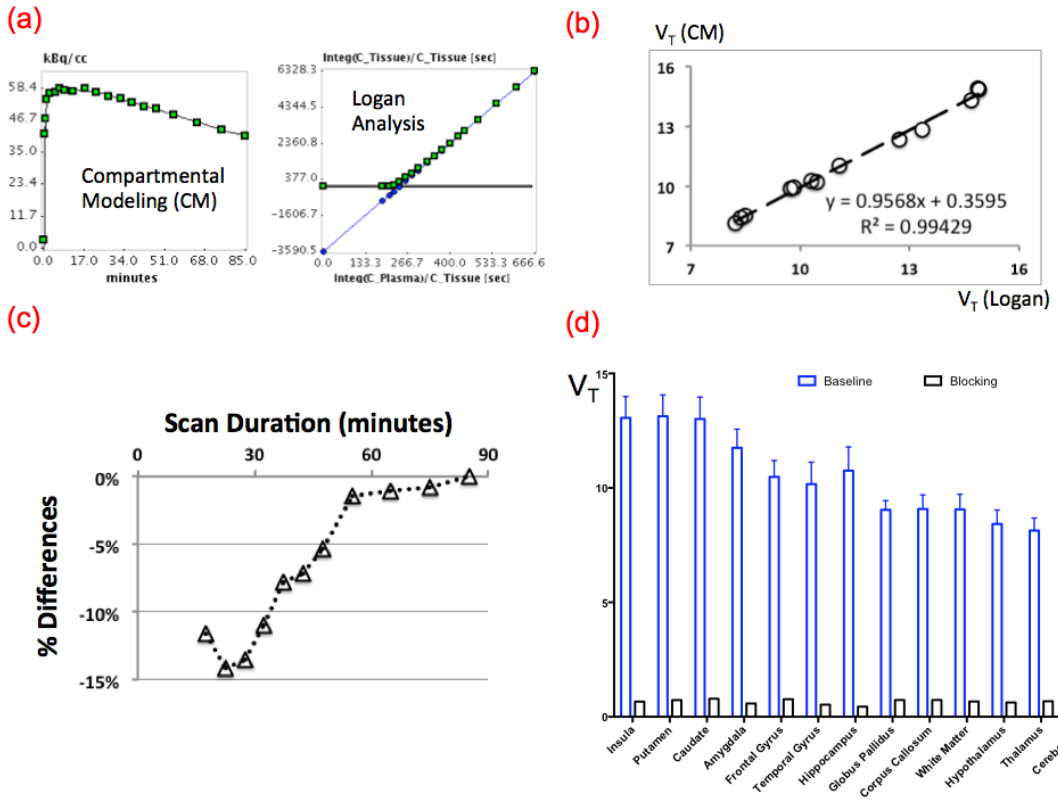

Supplemental Figure 3. (a) Representative plots of ^{18}F-FNDP kinetic analysis using both compartmental modeling and Logan analysis, demonstrating both are suitable methods (representative region shown: putamen, green markers: PET study data points, solid lines: fitted data; (b) Comparisons of V_T results by compartmental modeling and Logan analysis, in a representative baseline study, demonstrating they are highly comparable/correlated (R^2=0.99); (c) Representative time-consistency plots of regional V_T estimates (region: putamen), showing stable results (<2% changes) were obtained starting 60 min post injections; (d) Comparisons of ^{18}F-FNDP PET regional distribution volume (V_T, by Logan analysis) between baseline and blocking scans in the baboon brain for 13 brain regions. Data = mean V_T ± SD (baseline n = 3, blocking n = 1)

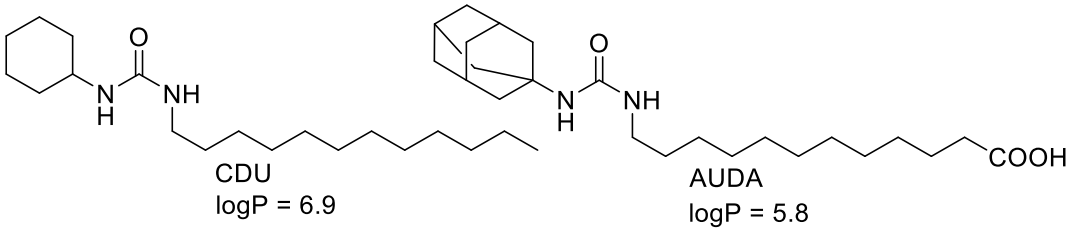

Supplemental Figure 4. 1-Cyclohexyl-3-dodecyl-urea (CDU) and 12-(3-(adamantan-1-yl)ureido)dodecanoic acid (AUDA) are representative sEH inhibitors (*2*). Because of the large hydrophobic domains in their structures these compounds are considered unsuitable leads for PET radiotracer development.

Baboon PET studies

Three male baboons (*Papio anubis*) were scanned at baseline using the High Resolution Research Tomograph (HRRT, CPS Innovations, Inc., Knoxville, TN). One of the baboons, weighing 28.2 kg, also underwent a blocking scan 3 weeks later. For each scan, the animal was fasted for 12 h prior to PET study. Anesthesia was induced with intramuscular ketamine (7.5-10 mg/kg) and maintained with a continuous intravenous infusion of propofol at 0.3-0.4 mg/kg/min throughout the PET experiment. One venous catheter was inserted for the radioligand injection, and one arterial catheter inserted to obtain arterial blood samples. Measurement of the arterial plasma input function was conducted through collection of 43 blood samples over the course of the 90 min dynamic PET scan. The baboon was also intubated to facilitate respiration, and circulatory volume was maintained by constant infusion of isotonic saline. Physiological vital signs including heart rate, blood pressure, electrocardiogram, and oxygen saturation were monitored continuously throughout the study.

Each animal was positioned in the PET scanner with the head immobilized with a thermoplastic mask. A 6 min transmission scan was acquired using a rotating [^{137}Cs]cesium source for attenuation correction. The 90-min dynamic PET acquisition was then started in three-dimensional list mode simultaneously with an intravenous bolus injection of ^{18}F-FNDP. For the blocking scan, nor-fluoro-FNDP (2 mg/kg) was given subcutaneously 1 h prior to the intravenous bolus injection of ^{18}F-FNDP and the start of the 90-min dynamic PET imaging.

***PET Image Reconstruction*:** The 90 min PET list mode data were binned into 22 frames (three 20 s, two 30 s, two 1 min, three 2 min, eight 5 min, and four 10 min frames). The data were then reconstructed using the iterative ordered subsets expectation maximization (OS-EM) algorithm (with six iterations and 16 subsets), with correction for radioactive decay, dead time, attenuation, scatter and randoms. The attenuation maps were generated from 6 min transmission scans performed with a [^{137}Cs]cesium point source prior to the emission scans. The reconstructed image space consisted of cubic voxels, each 1.22 mm^3 in size, and spanning dimensions of 31 cm x 31 cm (transaxially) and 25 cm (axially).

***Brain volumes of interest (VOIs) and regional time-activity curves (TACs)*:** The software package PMOD (v3.3, PMOD Technologies Ltd, Zurich, Switzerland) was used for the following image processing and subsequent kinetic analysis steps. The previously acquired brain MRI T1-weighted images for the baboon

were co-registered to the reconstructed dynamic PET images acquired in this study. Through manually matching the co-registered MRI to the INIA19 Template and NeuroMaps Atlas for Primate Brain Image Parcellation and Spatial Normalization (*4*), 13 representative baboon brain VOIs were defined, including frontal and temporal gyrus, thalamus, hippocampus, caudate, putamen, amygdala, globus pallidus, insula, hypothalamus, cerebellum, corpus callosum, and white matter. Brain regional TACs were then generated for both baseline and blocking PET scans using those VOIs.

PET kinetic analysis: calculation of brain regional distribution volume (V_T): Based on the regional TACs obtained above, ^{18}F-FNDP binding to sEH was quantitatively characterized with the use of the metabolite-corrected arterial plasma input function. Following the consensus nomenclature for in vivo imaging of reversibly binding radioligands (*5*), due to the lack of a non-displaceable reference region, the main outcome measure was regional distribution volume (V_T), defined as the ratio of the concentration of the radioligand in regional brain tissue to that in plasma at equilibrium. Regional V_T is proportional to the receptor density in the defined VOI. V_T was calculated using both compartmental modeling and the Logan graphical method for each VOI (*6*). Time-consistency analysis was also performed. In Supplemental Figure 3, we presented representative results. In summary, both compartmental modeling and Logan method are suitable for analyzing the ^{18}F-FNDP PET data (example shown in Suppl. Fig. 3-a), and they generated very comparable regional V_T results (Suppl. Fig. 3-b). All brain regions yielded stable V_T estimates for scan durations longer than 60 minutes (Suppl. Fig. 3-c). To facilitate obtaining V_T parametric images (Fig. 6 in the manuscript), we chose the Logan method for presenting all V_T values in the manuscript. The Suppl. Fig. 3-d demonstrated the regional V_T comparisons between 3 baseline scans and the one blocking scan.

Radiometabolite HPLC analysis: Baboon arterial blood samples were collected at very short intervals (< 5 s) initially and gradually at prolonged intervals throughout the PET study for determination of plasma radioactivity. Selected samples taken at 0, 5, 10, 20, 30, 60, and 90 min were analyzed by HPLC for the presence of ^{18}F-FNDP and its radioactive metabolites (Supplemental Figure 5) using the general method described previously (*3*). Briefly, 3 mL of plasma in 8 M urea was passed through a capture column (19 x 4.6 mm Strata-X, Phenomenex, Torrance, CA), followed by 1% acetonitrile in water to wash plasma proteins from the column. The effluent from the capture column, containing only highly polar components, flowed through a dual BGO detector (Bioscan, Washington, DC). The solvent was then switched to a mixture of 60% acetonitrile/40% 0.1M aqueous ammonium formate pH = 2.7 (2 mL/min) to elute the radiolabeled components bound to the capture column onto the analytical column (Gemini C18, 4.6 x 254 mm, Phenomenex, Torrance, CA).

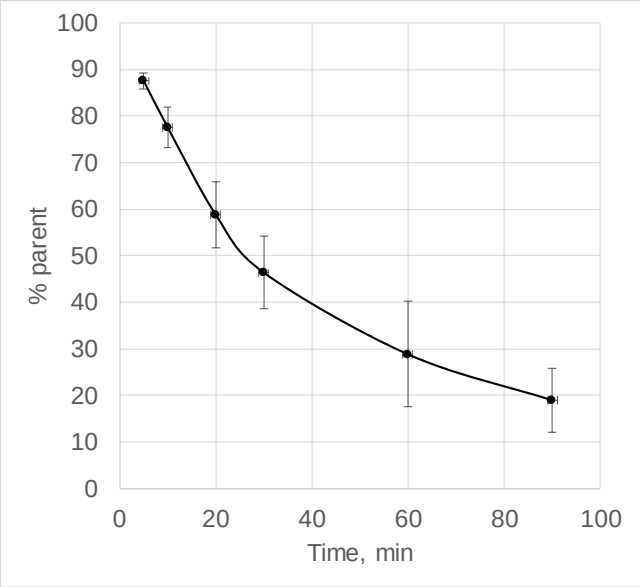

Supplemental Figure 5. HPLC radiometabolite analysis, time-% curve of parent ^{18}F-FNDP in baboon plasma. Data = mean %parent ± SD, n = 3.

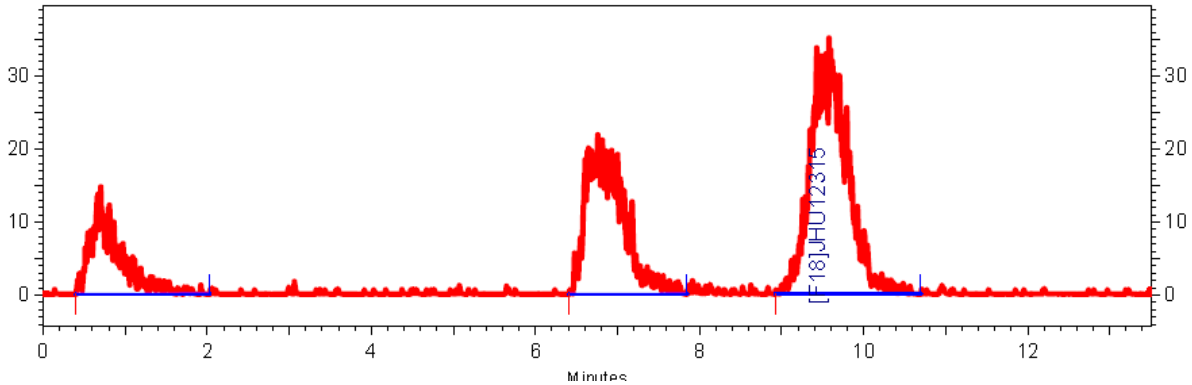

Supplemental Figure 6. Representative radiometabolite HPLC of baboon plasma, 60 min time-point (parent ^{18}F-FNDP (^{18}F-JHU12315) – 9.5 min, two radiometabolites – 0.7 and 6.8 min)

Supplemental Data References

1. Eldrup AB, Soleymanzadeh F, Taylor SJ, et al. Structure-based optimization of arylamides as inhibitors of soluble epoxide hydrolase. *J Med Chem.* 2009;52:5880-5895.

2. Shen HC. Soluble epoxide hydrolase inhibitors: a patent review. *Expert Opin Ther Pat.* 2010;20:941-956.

3. Hilton J, Yokoi F, Dannals RF, Ravert HT, Szabo Z, Wong DF. Column-switching HPLC for the analysis of plasma in PET imaging studies. *Nucl Med Biol.* 2000;27:627-630.

4. Rohlfing T, Kroenke CD, Sullivan EV, et al. The INIA19 Template and NeuroMaps Atlas for Primate Brain Image Parcellation and Spatial Normalization. *Frontiers in neuroinformatics.* 2012;6:27.

5. Innis RB, Cunningham VJ, Delforge J, et al. Consensus nomenclature for in vivo imaging of reversibly binding radioligands. *J Cereb Blood Flow Metab.* 2007;27:1533-1539.

6. Logan J, Fowler JS, Volkow ND, et al. Graphical analysis of reversible radioligand binding from time-activity measurements applied to [N-11C-methyl]-(-)-cocaine PET studies in human subjects. *J Cereb Blood Flow Metab.* 1990;10:740-747.